line as other primary amines for reaction with *p*-nitrophenyl phosphate dianion and phosphorylated isoquinoline monoanion.[17,28] (5) Nicotinate anion falls on the same Brønsted correlation line as uncharged pyridines for reaction with phosphorylated pyridine monoanions.[16] An apparent exception is the ≥8-fold decrease in the reactivity of nicotinate anion compared with uncharged pyridines for reaction with 2,4-dinitrophenyl phosphate dianion.[5,66] The reason for this is not clear, but it may involve an unfavorable interaction between an oxygen atom of the constrained meta carboxylate group of nicotinate with an oxygen atom of the phosphoryl group. Inspection of CPK molecular models suggests that the distance between the phosphoryl oxygen atoms and the carboxylate oxygen atoms of glycine and of nicotinate is nearly the same in the two transition states, but the glycine carboxylate group is free to move to a position in which it is pointed away from the phosphoryl group.

(65) It has been suggested that rate constants for reactions of phosphoryl compounds with monocations of Dabco and piperazine may be greater than expected, as a result of electrostatic attraction: Lloyd, G. J.; Hsu, C.-M.; Cooperman, B. S. *J. Am. Chem. Soc.* **1971**, *93*, 4889-4892; ref 64. However, Brønsted-type correlations that support rate constants that are greater than predicted have not been reported.

(66) No reaction of nicotinate anion with dinitrophenyl phosphate dianion was observed. A maximum rate constant for the reaction of 7.0×10^{-5} M^{-1} s^{-1} at 39 °C was taken from the smallest observed rate constant in Table I of ref 5.

Neutron Profile Refinement of the Structure of FeOCl and $FeOCl(TTF)_{1/8.5}$

S. M. Kauzlarich,[†,‡] J. L. Stanton,[‡] J. Faber, Jr.,[⊥] and B. A. Averill*[‡]

Contribution from the Department of Chemistry, University of Virginia, Charlottesville, Virginia 22901, Department of Chemistry, Michigan State University, East Lansing, Michigan 48824, and Argonne National Laboratory, Argonne, Illinois 60439. *Received April 11, 1986*

Abstract: Neutron diffraction studies on powder samples of FeOCl and $FeOCl(TTF)_{1/8.5}$ establish that TTF intercalated into FeOCl contributes to the diffraction pattern and exhibits long-range order. Room-temperature time-of-flight diffraction results are reported. The structure of FeOCl was refined in a space group *Pmnm* with $a = 3.7730$ (1) Å, $b = 7.9096$ (1) Å, and $c = 3.3010$ (1) Å. Least-squares Rietveld refinement (21 parameters, 3296 degrees of freedom) yielded $R = 0.0169$, $R_w = 0.0248$ ($R_{expected} = 0.0115$). The structure of $FeOCl(TTF)_{1/8.5}$ was refined in space group *Immm* with $a = 3.784$ (2) Å, $b = 3.341$ (2) Å, and $c = 25.97$ (2) Å, using a model in which the TTF molecules lie in the *bc* plane, with equal occupancy of the four possible sites, to give $R = 0.0203$, $R_w = 0.0289$, and $R_{expected} = 0.0111$ (28 parameters, 1894 degrees of freedom).

Intercalation compounds are of interest not only as catalytic materials[1] but also as low-dimensional conductors.[2] Neutron diffraction studies on TaS_2- and NbS_2-pyridine intercalates[3] showed that the aromatic ring is perpendicular to the host layers and that the C-N axis of the pyridine ring is oriented parallel to the sulfide layers. This result was contrary to initial ideas that the nitrogen lone pair was directed at metal atoms within the host or that the pyridine rings were parallel to the host layers.[4] A structure similar to that of $NbS_2(py)_{0.5}$ (py = pyridine) has been proposed for $FeOCl(py)_{1/3}$.[5] Structural models have been proposed for amine intercalates of FeOCl and other metal oxychlorides based on lattice expansions and Mössbauer,[5,6] NMR,[7] and pseudo-single-crystal[8] studies. The currently accepted model is one in which the threefold axis of the amine is not parallel to the *b* axis of the host, and the amines are "nested" in the chloride layers.[7a]

A new class of intercalates currently under investigation in our laboratory employs tetrathiafulvalene (TTF) and related compounds as guest species.[2,9] A layered material such as FeOCl has the potential to enforce a self-stacked structure upon the intercalated electron-donor molecules, a requirement for low-dimensional conductors.[10] In addition, charge transfer occurs between the tetrathiolene guest and the host lattice, resulting in stacks of radical cations between the layers.[9] Iron K-edge EXAFS (extended X-ray absorption fine structure) spectra show little perturbation of the local Fe environment in the intercalates,[11] indicating that the structure of the host layers has not changed significantly. Powder X-ray diffraction data confirm the existence

* To whom correspondence should be addressed.
[†] Michigan State University.
[‡] University of Virginia.
[⊥] Argonne National Laboratory.

(1) *Intercalation Chemistry*; Whittingham, M. S., Jacobson, A. J., Eds.; Academic: New York, 1982.
(2) Averill, B. A.; Kauzlarich, S. M. *Mol. Cryst. Liq. Cryst.* **1984**, *107*, 55-64.
(3) (a) Riekel, C.; Hohlwein, D.; Schollhorn, R. *J. Chem. Soc., Chem. Commun.* **1976**, 863-864. (b) Riekel, C.; Fischer, C. O. *J. Solid State Chem.* **1979**, *29*, 181-190.
(4) (a) Gamble, F. R.; DiSalvo, F. J.; Klemm, R. A.; Geballe, T. H. *Science* **1970**, *168*, 568-570. (b) Gamble, F. R.; Osieck, J. H.; DiSalvo, F. J. *J. Chem. Phys.* **1971**, *55*, 3525-3530.
(5) Eckert, H.; Herber, R. H. *J. Chem. Phys.* **1984**, *80*, 4526-4540.
(6) (a) Kanamaru, F.; Shimada, M.; Koizumi, M.; Takano, M.; Takada, T. *J. Solid State Chem.* **1973**, *7*, 297-299. (b) Kikkawa, S.; Kanamaru, F.; Koizumi, M. *Physica* **1981**, *105B*, 249-252. (c) Kikkawa, S.; Kanamaru, F.; Koizumi, M. *Bull. Chem. Soc. Jpn.* **1979**, *52*, 963-966. (d) Maeda, Y.; Yamashita, M.; Ohshio, H.; Tsutsumi, N.; Takashima, Y. *Bull. Chem. Soc. Jpn.* **1982**, *55*, 3138-3143. (e) Herber, R. H. *Acc. Chem. Res.* **1982**, *15*, 216-224. (f) Herber, R. H.; Maeda, Y. *Inorg. Chem.*, **1981**, *20*, 1409-1415. (g) Fatseas, G. A.; Palvadeau, P.; Venien, J. P. In *Solid State Chemistry*, Processings of the 2nd European Congress, Veldhoven, The Netherlands, June 7-9 1982. Metselaar, R., Heijligers, H. J. M., Schoonman, J., Eds. *Studies in Inorganic Chemistry*; Elsevier: Amsterdam, 1983; Vol. 3, pp 627-630.
(7) (a) Rouxel, J.; Palvadeau, P. *Rev. Chim. Min.* **1982**, *19*, 317-332. (b) Clough, S.; Palvadeau, P.; Venien, J. P. *J. Phys. C: Solid State Phys.* **1982**, *15*, 641-655.
(8) Fatseas, G. A.; Palvadeau, P.; Venien, J. P. *J. Solid State Chem.* **1984**, *51*, 17-37.
(9) (a) Antonio, M. R.; Averill, B. A. *J. Chem. Soc., Chem. Commun.* **1981**, 382-383. (b) Averill, B. A.; Kauzlarich, S. M.; Antonio, M. R. *J. de Phys. (Paris)* **1983**, *44* C3-1373-C3-1376. (c) Kauzlarich, S. M.; Averill, B. A.; Teo, B. K. *Mol. Cryst. Liq. Cryst.* **1984**, *107*, 65-74. (d) Averill, B. A.; Kauzlarich, S. M.; Teo, B. K.; Faber, J., Jr. *Mol. Cryst. Liq. Cryst.* **1985**, *120*, 259-262.

0002-7863/86/1508-7946$01.50/0

Table I. Cell Parameters and Final Positional and Thermal Parameters for FeOCl at 300 K

	a (Å) 3.7730 (1)		*b* (Å) 7.9096 (1)		*c* (Å) 3.3010 (1)	
	x	*y*	*z*	$B_{xx}(10^3)$	$B_{yy}(10^3)$	$B_{zz}(10^3)$
Fe	0.25	0.115 55 (8)	0.75	13.8 (4)	6.2 (1)	14.6 (5)
O	0.25	−0.047 95 (15)	0.25	10.7 (6)	7.35 (2)	17.6 (8)
Cl	0.25	0.329 61 (7)	0.25	43.8 (6)	5.6 (5)	19.8 (1)
	R = 0.0169		R_w = 0.0249		$R_{expected}$ = 0.0115	

of long-range order and the crystallinity of the solid,[11] but they are dominated by the FeOCl layers. Unfortunately, neither EXAFS nor X-ray powder diffraction provides direct information on the position and orientation of the TTF guest.

The independence of neutron scattering power upon atomic number makes neutron powder diffraction a promising technique for elucidating the structure of FeOCl(TTF)$_{1/8.5}$. Neutron diffraction data are complementary to the X-ray data and have provided the first evidence for long-range ordering of the TTF radical cations within FeOCl. The study required high neutron flux, a large data collection range (10–0.5 Å), and resolution comparable to that of an X-ray powder experiment.

Experimental Section

FeOCl was prepared[6c] by reaction of α-Fe_2O_3 with excess $FeCl_3$ at 370 °C for 1 week in a sealed, evacuated tube (quartz or Pyrex). Excess $FeCl_3$ was removed by washing with acetone that had been dried over $CaSO_4$ and degassed. The intercalate was prepared by reaction of FeOCl with TTF in dimethoxyethane for 10 days at 60 °C.[9] The dimethoxyethane was distilled from CaH_2. Both FeOCl and FeOCl(TTF)$_{1/8.5}$ are water-sensitive, and all manipulations were carried out under a nitrogen atmosphere. The samples were characterized by X-ray powder diffraction and elemental analyses.

Neutron powder diffraction data were collected on the General Purpose Powder Diffractometer (GPPD) at the Intense Pulsed Neutron Source (IPNS) and analyzed at Argonne National Laboratory. IPNS uses a proton accelerator and synchrotron to produce high-energy neutrons by bombardment of a spallation target (uranium). These neutrons are then moderated to lower energies before they are used for diffraction. The GPPD is equipped with time-of-flight detectors, of which there are two sets each at 30°, 45°, 60°, 75°, 90°, and 150°. Highest resolution data are obtained from the 150° detector bank.[12] The samples (FeOCl and FeOCl(TTF)$_{1/8.5}$) were run at room temperature in a vanadium cell.

The neutron diffraction data obtained in the 2θ = 150° and 90° detector banks for FeOCl and FeOCl(TTF)$_{1/8.5}$, respectively, were used in the refinements. The Rietveld refinement of the time-of-flight data was performed with using a modified version of the original program written by Rietveld.[13] Two programs (TOFPRP, TOFLS) fit the background, peak shape, and scaling factors and perform a full-matrix least-squares refinement of the crystal structure.[14,15] The refinement is achieved by minimizing the sum of the squares of the weighted differences between the observed and calculated intensities for every point in the profile under the Bragg reflections by adjusting the structural and profile parameters.

The initial atomic positions for the unit cell of FeOCl were taken from the single-crystal X-ray study.[16] The FeOCl structure was refined satisfactorily (R = 0.0169, R_w = 0.0248, $R_{expected}$ = 0.0115), varying 21 parameters in the final refinement (3296 degrees of freedom). The refined parameters were two background parameters, two half-width parameters, extinction, cell constants, a scale factor, and atomic positional and anisotropic thermal parameters.

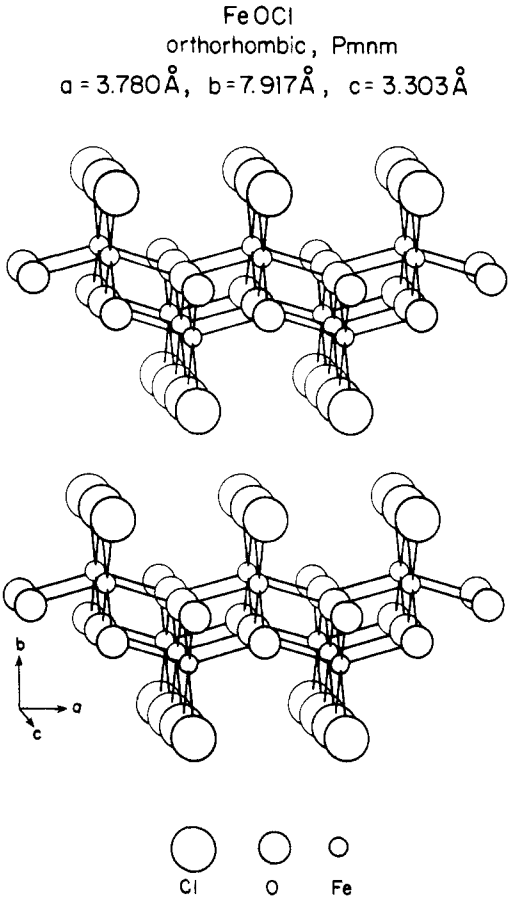

Figure 1. Perspective view of two layers of the FeOCl structure. FeOCl is orthorhombic, *Pmnm*, a = 3.780 Å, b = 7.917 Å, c = 3.303 Å. Figure adapted from ref 17.

The structure of FeOCl(TTF)$_{1/8.5}$ was initially refined with Fe, O, and Cl atomic positions calculated from an idealized model[11] and a limited range of data (1.359–5.0 Å, 1428 degrees of freedom). A difference Fourier synthesis showed significant nuclear density between the host layers. Subsequent refinements were carried out with a model that includes a TTF molecule intercalated into the FeOCl host. Since one molecule of TTF spans four unit cells of the host lattice along c, atomic positions for C, S, and H were obtained by the superposition (at 1/4 occupancy) of C, S, and H positions in the four unit cells. The final refinement used a larger data range (0.766–3.515 Å, 1984 degrees of freedom). The programs used for final refinement were TPRNEW and TLSMOD, recent modifications[14b] of the programs used in earlier refinements, which allow refinement of a 5-parameter background function and a 3-parameter line width function.

Results and Discussion

FeOCl. The FeOCl structure consists of a stacked neutral layers of distorted *cis*-$(FeCl_2O_4)^{7-}$ octahedra, which share half their edges to produce a central sheet of $(FeO)_n$ with Cl^- layers outermost on either side of the sheet.[14] The iron atoms share a single atom along the a axis and both an oxygen and a chlorine atom along the c axis (Figure 1). FeOCl crystallizes in an orthorhombic space group, *Pmnm*. The refined cell parameters and atomic positional and thermal parameters are given in Table I. Figure 2 compares one section of the experimentally determined neutron diffraction pattern and the pattern calculated with the parameters given in Table I. The cell parameters obtained in the refinement are in

(10) (a) Hoffman, B. M.; Ibers, J. A. *Acc. Chem. Res.* **1983**, *16*, 15–21. (b) Bryce, M. R.; Murphy, L. C. *Nature (London)* **1984**, *309*, 119–126. (c) Lyubovskaya, R. N. *Russ. Chem. Rev.* **1983**, *52*, 736–750. (d) Williams, J. M.; Beno, M. A.; Wang. H. H.; Leung, P. C. W.; Enge, T. J.; Geiser, U.; Carlson, K. D. *Acc. Chem. Res.* **1985**, *18*, 261–267. (e) Wudl, F. *Ibid.* **1984**, *17*, 227–232.

(11) Kauzlarich, S. M.; Teo, B. K.; Averill, B. A. *Inorg. Chem.* **1986**, *25*, 1209–1215.

(12) IPNS Progress Report, Argonne National Laboratory, Argonne, IL, 1981–1983; pp 2–40.

(13) Rietveld, H. M. *J. Appl. Crystallogr.* **1969**, *2*, 65–71.

(14) (a) Rotella, F. J. *Users Manual for Rietveld Analysis of Time-of-Flight Neutron Diffraction Data at IPNS*; Argonne National Laboratory: Argonne, IL, 1983. (b) Rotella, F. J. *Notes on the Rietveld Analysis of Time-of-Flight Neutron Diffraction Powder Data Using TLSMOD*; Argonne National Laboratory: Argonne, IL, 1985.

(15) Von Dreele, R. B.; Jorgensen, J. D.; Windsor, C. G. *J. Appl. Crystallogr.* **1982**, *15*, 581–589.

(16) Lind, M. D. *Acta Crystallogr.* **1970**, *B26*, 1058–1062.

(17) Halbert, T. R., in ref. 1, pp 375–403.

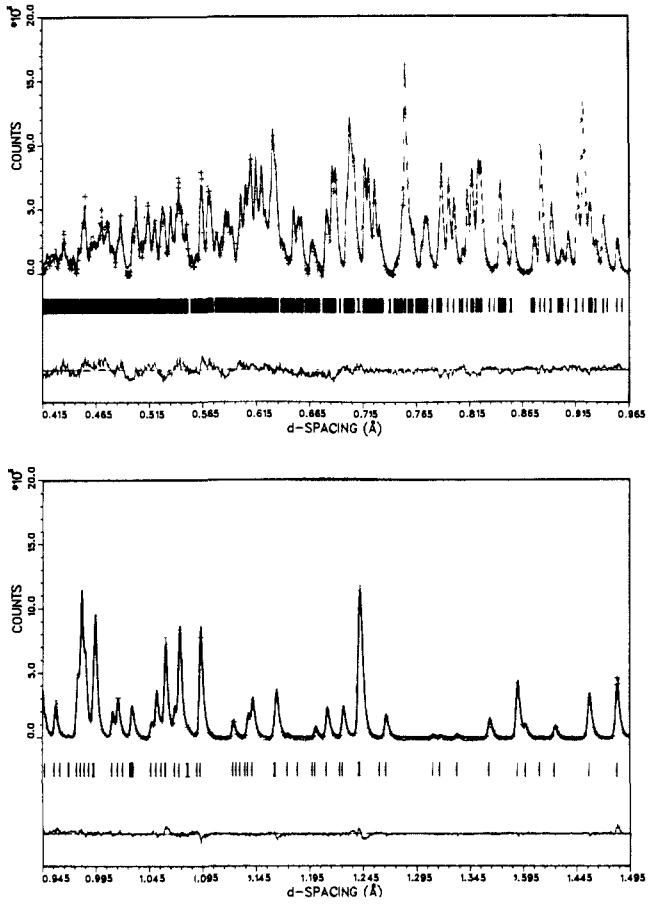

Figure 2. Profile refinement of a portion of the 150° bank data for FeOCl at 300 K. The observed data are indicated by points and the calculated data by a solid line. Marks directly beneath the pattern indicate the positions of reflections. A difference curve appears at the bottom.

Table II. Distances and Angles Obtained for FeOCl (There Are 2 FeOCl Formula Units per Unit Cell)

	distance (Å)	no. in unit cell
Fe—O	1.9608 (5)	8
Fe—O	2.0968 (9)	8
Fe—Cl	2.3645 (8)	8
Fe···Fe	3.1023 (8)	16
Fe···Fe	3.3010 (1)	8
Fe···Fe	3.7730 (1)	8
Fe···O	3.8395 (3)	16
Fe···Cl	3.9946 (9)	8
	angle (deg)	
O–Fe–O	103.84 (7)	
O–Fe–O	80.32 (3)	
O–Fe–Cl	83.81 (4)	
O–Fe–Cl	172.35 (5)	
Cl–Fe–Cl	88.35 (5)	
O–Fe–Cl	101.26 (4)	
O–Fe–O	148.35 (9)	

good agreement with those reported by Rouxel and Palvadeau,[7a] but are more precise. The chlorine atoms exhibit relatively large thermal parameters along both the *a* and *c* axes, consistent with weak interlayer interactions and the ease of intercalation by Lewis bases. Selected interatomic distances and angles are given in Table II.

FeOCl(TTF)$_{1/8.5}$. For FeOCl intercalated with TTF, a number of constraints must be considered before a Rietveld profile analysis can be undertaken. The Rietveld method is a technique for structure refinement, not structure determination. The basic structure must be known (or guessed at) before the data can be fit.

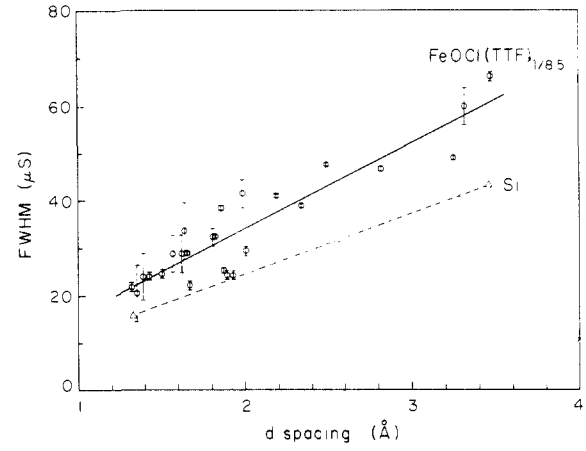

Figure 3. Plot of full width at half-maximum (fwhm) of diffraction peaks of FeOCl(TTF)$_{1/8.5}$ compared with a standard silicon sample. Differences in particle size and residual strains are reflected in different slope and intercept values of the two samples. The monotonic rise in fwhm values for FeOCl(TTF)$_{1/8.5}$ indicates that all Bragg reflections in this d-spacing range have been detected.

Table III. Cell Constants and Figures of Merit Obtained for Twenty Reflections from Neutron Powder Diffraction Data for FeOCl(TTF)$_{1/8.5}$

a (Å)	*b* (Å)	*c* (Å)	figure of merit	unit cell volume (Å^3)
3.784	25.961	3.341	1614.9	328.17
10.016	12.986	3.854	14.2	501.31
6.688	25.959	4.585	11.5	796.02

To begin the analysis it was necessary to identify and index all the Bragg reflections in the powder pattern. The Bragg peaks were fit with TOFMANY,[18] a multiplet peak-fitting program. The peak shape is computed from the profile parameters of the diffracted peaks by the convolution of a Gaussian peak with a hypothetical pulse shape composed of a rising exponential leading edge and a decaying exponential trailing eedge.[15,18] Full widths at half-maximum height (fwhm) were compared to those of the instrument's calibration material, silicon (Figure 3). The diffracted peaks for FeOCl(TTF)$_{1/8.5}$ are broader than those of silicon, indicating that the intercalate may have small lattice strains resulting from intercalation, and that the mean particle size is smaller than for silicon. A good correspondence between the plots is observed, indicating that all Bragg reflections, including those in multiple peak groups, have been accounted for by the indexing scheme.

The peaks were indexed by a computer-based method (TOFIDX).[14,19] Although there is usually not a unique solution, the program gives figures of merit that strongly discriminate between the solutions. A minimum of 20 Bragg reflections is necessary to obtain reliable results. Twenty experimental reflections whose peak positions had been determined from the peak fitting program were used. Three solutions were found by the indexing program for an orthorhombic cell (Table III). A large figure of merit indicates a good fit; solutions with figures of merit less than 4 were disregarded. In Table IV, the experimental *d*-spacings are compared to those calculated for the orthorhombic cell with the largest figure of merit.

The structural model used for the FeOCl layers of the intercalate results from translating alternate FeOCl layers by $^1/_2$, 0, $^1/_2$) and expanding the interlayer gap to accommodate the TTF molecules. The resulting symmetry necessitates a doubling of the *b* axis to form a centered unit cell (Figure 4). Such translations of the host layers and increases in interlayer distances have been observed upon intercalation of FeOCl and other layered hosts.[5,7a] A more standard unit cell description[20] (with *c* as the long axis)

(18) Faber, J., Jr.; Hitterman, R. L. *Adv. X-ray Anal.* **1986**, *29*, 119–130.
(19) Visser, J. W. *J. Appl. Crystallogr.* **1969**, *2*, 89–95.

Table IV. Observed and Calculated d-Spacings (Å) of the Neutron Powder Diffraction Data for FeOCl(TTF)$_{1/8.5}$ with the Proposed Indexing Scheme: a = 3.7836 (4) Å, b = 25.9629 (3) Å, and c = 3.341 (4) Å

d_{obsd} (Å)	h	k	l	d_{calcd} (Å)
3.4676 (1)	1	3	0	3.4667
3.3128 (7)	0	1	1	3.3137
3.2452 (5)	0	8	0	3.2452
2.8099 (4)	0	5	1	2.8096
2.4827 (1)	0	7	1	2.4823
2.3366 (1)	1	4	1	2.3365
2.1834 (1)	0	9	1	2.1834
2.0029 (4)	1	11	0	2.0025
1.9828 (4)	1	8	1	1.9826
1.9280 (5)	0	11	1	1.9277
1.8918 (1)	2	0	0	1.8918
1.8720 (1)	2	2	0	1.8720
1.8551 (2)	0	14	0	1.8544
1.8157 (5)	2	4	0	1.8162
1.8026 (1)	1	10	1	1.8024
1.6705 (3)	0	0	2	1.6705
1.6566 (3)	0	2	2	1.6568
1.6377 (1)	1	12	1	1.6372
1.6220 (1)	0	16	0	1.6226
1.5701 (1)	2	5	1	1.5692
1.5049 (1)	1	3	2	1.5049
1.4301 (1)	2	9	1	1.4298
1.4164 (1)	1	17	0	1.4161
1.4055 (3)	0	10	2	1.4048
1.3893 (2)	0	12	1	1.3889
1.3509 (4)	1	9	2	1.3504
1.3241 (1)	0	18	1	1.3242

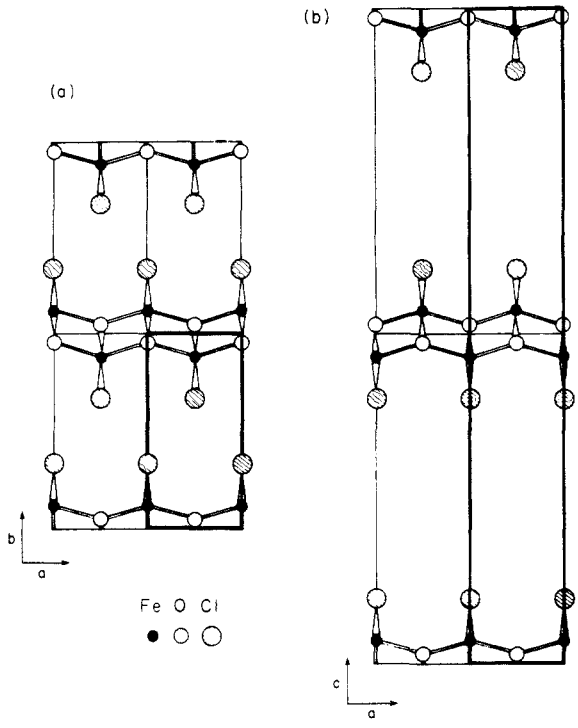

Figure 4. Projection of the unit cell of FeOCl showing the change in cell symmetry that accompanies cell expansion upon intercalation.

was employed in space group *Immm* for the remainder of the refinement. Initial atomic positions for Fe, O, and Cl were calculated on the basis of the structure of FeOCl. A least-squares refinement of 14 parameters over a limited data range (1310 degrees of freedom) with only Fe, O, and Cl atoms resulted in the following R factors: R = 0.0609, R_w = 0.0892, $R_{expected}$ = 0.0190; the fit to a portion of the experimental data is shown in Figure 5. A difference Fourier synthesis was performed on the observed and calculated structure factor amplitudes. The resulting Fourier difference map showed significant nuclear density between the FeOCl layers. This indicates that the TTF molecules contribute to the long-range order in FeOCl(TTF)$_{1/8.5}$.

The presence of TTF in the unit cell was modelled by superimposing, at 1/4 occupancy, the atomic positions of the C, S, and H atoms of TTF in each of the four unit cells spanned by a TTF molecule. Upon inclusion of the TTF in the model, the data range that could be fit in the least-squares refinement expanded to 1894 degrees of freedom, and the R factors decreased substantially to R = 0.0203, R_w = 0.0289, $R_{expected}$ = 0.0111. One portion of the fit to the experimental data is shown in Figure 6, while Table V gives the final refined atomic and cell paramters.

The goodness of the final fit to the data leads to the conclusion that the TTF molecules must be aligned in the *bc* plane, perpendicular to the FeOCl layers as shown in Figure 7. This configuration locks the FeOCl layers into an eclipsed configuration

(20) For FeOCl(TTF)$_{1/8.5}$: a = 3.7841 (2) Å, b = 3.3407 (2) Å, c = 25.972 (2) Å, V = 328.32 (2) Å^3, Z = 4, space group *Immm*. Note that the b axis in this unit cell corresponds to the c axis of pristine FeOCl, while the interlayer distance is taken as c (rather than b in FeOCl).

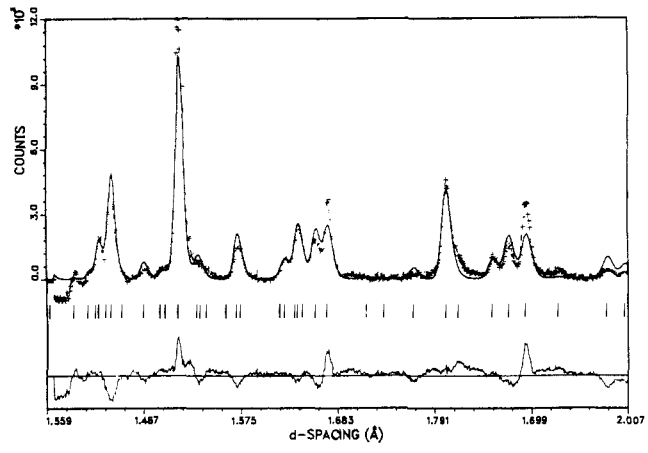

Figure 5. A portion of the profile refinement for FeOCl(TTF)$_{1/8.5}$, using a model that contains only Fe, O, and Cl atoms.

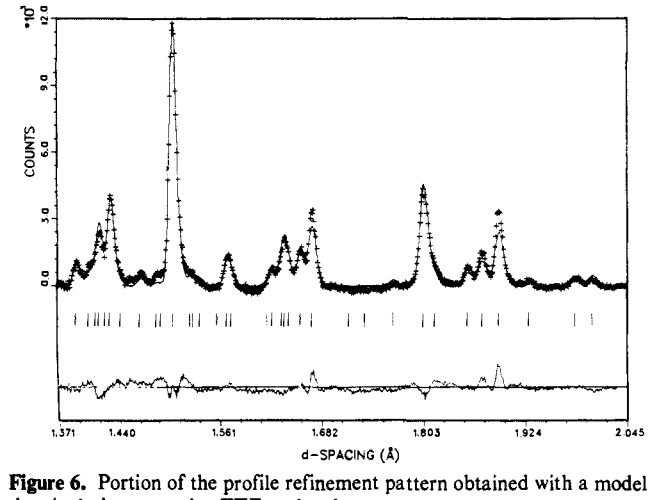

Figure 6. Portion of the profile refinement pattern obtained with a model that includes an entire TTF molecule.

Table V. Atomic Positions and Thermal Parameters for FeOCl(TTF)$_{1/8.5}$

atom	x	y	z	B
Fe	0.0	0.0	0.2170 (1)	1.35 (6)
O	0.5	0.0	0.2345 (2)	1.60 (9)
Cl	0.0	0.5	0.1487 (1)	1.82 (7)
S	0.5	−0.064 (15)	0.0599 (2)	1.05[a]
C(1)	0.5	0.358 (18)	0.0	1.04[a]
C(2)	0.5	0.539 (8)	0.249 (7)	1.36[a]
H	0.5	0.242 (11)	0.678 (18)	1.04[a]

[a] Isotropic thermal parameters for the atoms of TTF were held fixed at these values during the least-squares refinement.

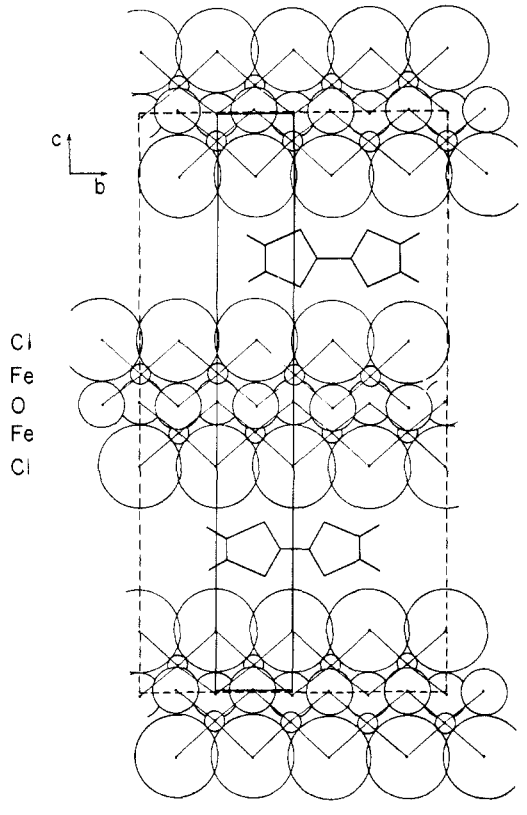

Figure 7. Orientation of one TTF molecule with respect to one unit cell (solid lines). A quadrupled unit cell along *b* (dashed lines) is required by the width of a TTF molecule.

and places the sulfur atoms of TTF rather close to the chlorine atoms of the FeOCl host (3.32 Å), well within the sum of the van der Waals radii (3.6 Å). We postulate that the nonbonded electron density on the sulfur atoms of TTF occupies approximately sp^3 orbitals directed *between* the chlorine atoms of FeOCl, thus minimizing repulsive S---Cl interactions. Similar arrangements of electron density have been deduced for the Se atoms in TMTSF derivatives based on electron density maps[21] and theoretical calculations.[22] Short S---Cl distances have also been recently observed for a number of TTF salts: e.g., [TMTTF][$FeCl_4$], 3.48 Å;[23] [dibenzoTTF]$_8$[$SnCl_6$]$_3$, 3.17, 3.39 Å;[24] [dibenzoTTF]$_2$[Cu_2Cl_6], 3.68–3.96 Å;[25] [TTF]$Cl_{0.92}$, 3.51 Å.[26] The above data suggest that relatively short S---Cl contacts are rather common, and need not imply the presence of an S---Cl bonding interaction. Indeed, we postulate exactly the opposite, that the sulfur approaches the chlorine along a line that *minimizes* S---Cl electronic interactions.

The structural model previously postulated[2,9b,c] for FeOCl-(TTF)$_{1/8.5}$ was based on the results of powder X-ray diffraction studies and assumed that the sulfur atoms of the intercalant interacted with the chlorine atoms of the host as hard spheres of fixed van der Waals radius. Because X-ray powder diffraction gives significantly fewer reflections than observed by neutron diffraction, the X-ray data were consistent with either of two models:[11] (a) a monoclinic unit cell in which the FeOCl layers remain staggered and the plane of the TTF molecule is oriented at an angle of 65° from the plane of the host layer; and (b) an orthorhombic unit cell in which the FeOCl layers are eclipsed, forcing the TTF to be oriented perpendicular to the layers. The present neutron diffraction data unambiguously show the latter model to be correct.

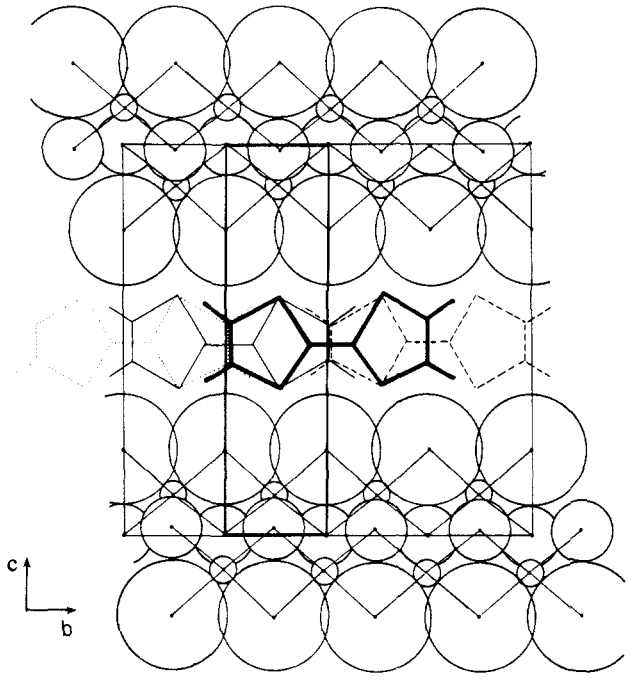

Figure 8. Four possible orientations of TTF within half of the defined unit cell (bold lines) and the quadrupled unit cell (dashed lines).

The model used here for TTF in FeOCl(TTF)$_{1/8.5}$ is a very general one, making no predictions about the specific stacking arrangement of the TTF molecules between the layers or in adjacent layers. The only restrictions on the TTF molecules are that they are perpendicular to the FeOCl layers and oriented along *b*. Disorder is used to take into account the four possible ways in which the TTF molecule may be arranged within a single orthorhombic unit cell of FeOCl (Figure 8). Obviously, the actual unit cell of the intercalate must include at least four of the unit cells defined in Figures 4 and 7. This structural model, in which the TTF molecule spans four unit cells along the *b* axis and one unit cell along the *a* axis, predicts a maximum stoichiometry of FeOCl(TTF)$_{1/8}$. This is in relatively good agreement with the experimentally determined stoichiometry of FeOCl(TTF)$_{1/8.5}$, allowing one unoccupied TTF site for every 16 occupied sites, and suggesting that the TTF molecules are approximately close packed within the layers. The random site model proposed here does not take this partial occupancy into account, nor does it specify the long-range arrangement of the TTF molecules. We calculate that there are sixteen possible different orientations of TTF molecules relative to one TTF molecule within the lattice that satisfy the symmetry requirements imposed by the data (the sixteen arrangements are the product of four different arrangements in the plane and four different arrangements out of the plane). Efforts are currently underway to resolve this problem with a combination of low-temperature data and data on the analogous perdeuterated intercalate, FeOCl(TTF-d_4)$_{1/8.5}$. In addition, solid-state NMR studies are in progress to probe the dynamics of the FeOCl–TTF interaction.

Conclusions

Analysis of neutron powder diffraction data has demonstrated that, upon intercalation of TTF, the *b* axis of FeOCl is expanded and doubled, resulting in a body-centered orthorhombic structure (space group *Immm* or I222). Both X-ray powder diffraction and EXAFS data[11] indicate that the intercalate is a well-defined solid with essentially undistorted FeOCl layers, thus supporting the hypothesis that the layers are locked by the intercalant. The neutron diffraction data indicate that the intercalated TTF

(21) Wudl, F.; Nalewajek, D.; Troup, J. M.; Extine, M. W. *Science* **1983**, *222*, 415–417.
(22) Grant, P. M. *Phys. Rev. B: Solid State* **1976**, *26*, 6888–6895.
(23) Batail, P.; Ouahab, L.; Torrance, J. B.; Pylman, M. L.; Parkin, S. S. P. *Solid State Commun.* **1985**, *55*, 597–600.
(24) Shibaeva, R. P.; Rozenberg, L. P.; Lobkovskaya, R. M. *Sov. Phys. Crystallogr. (Engl. Transl.)* **1980**, *25*, 292–295.
(25) Calculated from data in the following: Honda, M.; Katayama, C.; Tanaka, J.; Tanaka, M. *Acta Crystallogr. Sect. C: Cryst. Struct. Commun.* **1985**, *C41*, 197–199.
(26) Calculated from data in the following: Dahm, D. J.; Johnson, G. R.; May, F. L.; Miles, M. G.; Wilson, J. D. *Cryst. Struct. Commun.* **1975**, *4*, 673–676.

molecules contribute to the long-range order of the solid, and that they are perpendicular to the FeOCl layers and oriented along the *b* axis of the crystal (corresponding to the *c* axis of pristine FeOCl).

Acknowledgment. This research was supported by the National Science Foundation, Solid State Chemistry, Grant DMR-8313252 (B.A.A., S.M.K., J.L.S.), and in part by the Division of Basic Energy Sciences, U.S. Department of Energy (W-31-109-Eng-38). We thank IPNS for assistance with travel and lodging expenses and R. Hitterman for experimental assistance. B.A.A. was an Alfred P. Sloan Fellow, 1981-1985.

Registry No. FeOCl, 13870-10-5; $FeOCl(TTF)_{1/8.5}$, 100858-11-5.

Functionalized Keggin- and Dawson-Type Cyclopentadienyltitanium Heteropolytungstate Anions: Small, Individually Distinguishable Labels for Conventional Transmission Electron Microscopy. 1. Synthesis[1]

John F. W. Keana* and Marc D. Ogan

Contribution from the Department of Chemistry, University of Oregon, Eugene, Oregon 97403.
Received July 11, 1986

Abstract: With an eye toward the development of a new series of small, highly electron dense labels for electron microscopy, we have synthesized several cyclopentadienyltitanium-substituted Keggin- and Dawson-type heteropolytungstate (HPT) ions that bear reactive organic groups on the Cp ring suitable for selective attachment to macromolecular sites. R-Cp-$Ti(NMe_2)_3$ derivatives **5a-f** were prepared and then inserted into the Keggin defect HPT anion $PW_{11}O_{39}^{7-}$ **7** to give TBA salts **10a-e**. The major byproduct was shown to be oxotitanium compound **14**. Ion exchange of **10a-d** over acidic Al_2O_3 gave the corresponding moderately water soluble TMA salts **11**. Conventional ion exchange then gave the corresponding water soluble K^+ salts **13** and heteropoly acids **12**. Amine **10e** underwent methathetical exchange with $Cs_2B_{10}Br_{10}$ and then ion exchange to give **12e** and **13e**, from which **11e** was prepared. In the Dawson series, a suspension of HPT defect anion **16** in DMF was allowed to react with benzene solutions of **5c,e,f**, giving, after anion exchange on acidic alumina, the corresponding TMA salts **17a-c** which were then converted into K^+ salts **18a-c**. Oxotitanium HPT **21** was the major byproduct. Reaction of **16** with potassium bis(oxalato)oxotitanium(IV) also led to **21**, confirming the structure assignment. The new HPTs were characterized by elemental analysis of their TMA salts and by ^1H, ^{31}P, and ^{183}W NMR spectroscopy on the water soluble K^+ salts.

The direct visualization of cellular ultrastructure by electron microscopy (EM) is now possible routinely at near molecular resolution (<10 Å) and has contributed enormously to an understanding of cellular processes.[2] Central to the EM technique is the introduction of labels[3] of sufficient electron density to be detectable against the background matrix. The iron storage protein ferritin is the most widely used electron dense label. However, the large size of the ferritin-macromolecular complex and the uncertainty in the mode of attachment of the ferritin to the macromolecule limit the resolution to about 200-300 Å. Recognizing the need for new, smaller EM labels, Bartlett et al.[4] introduced the solubilized polycationic undecagold cluster $[(NH_2C_6H_4)_3P]_7Au_{11}(CN)_2$.[5] Progress has been made toward modification of the cluster for attachment to specific sites of interest[6] and structural results by using these are now becoming available.[7]

The synthesis of cyclopentadienyltitanium-substituted heteropolytungstate (HPT) **1** independently by Klemperer[8] and Knoth[9]

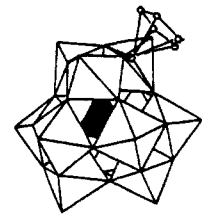

1 $CpTiPW_{11}O_{39}^{4-}$

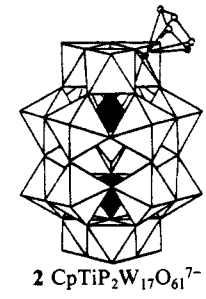

2 $CpTiP_2W_{17}O_{61}^{7-}$

and the ion's improved hydrolytic stability (up to pH ≃6) over the parent Keggin ion[10] suggested to us a new approach to EM labels, namely, the attachment of reactive organic functional groups to the cyclopentadienyl ring. Dawson-type[11] HPT ions derived from **2** offered the possibility of additional advantages in terms of stability at higher pH values and ease of detection in conventional transmission (CT) EM owing to the presence of 17 tungsten atoms within the ion. Herein, we report the synthesis and characterization of several Cp-substituted Keggin- and Dawson-type HPT ions that bear reactive organic groups suitable for chemoselective covalent bonding to macromolecular sites.[12] The accompanying paper[13] describes further chemical elaboration

(1) A preliminary account has appeared: Keana, J. F. W.; Ogan, M. D.; Lū, Y.; Beer, M.; Varkey, J. *J. Am. Chem. Soc.* **1985**, *107*, 6714.
(2) Hayat, M. A. *Principles and Techniques of Electron Microscopy. Biological Applications*, 2nd ed.; University Park Press: Baltimore, MD, 1981; Vol. 1.
(3) For a review, see: Hicks, D.; Molday, R. W. In *Science of Biological Specimen Preparation*; Revel, J.-P., Barnard, T., Haggis, G. H., Eds.; Scanning Electron Microscopy, Inc.: AMF O'Hare, IL, 1984; pp 203-219.
(4) Bartlett, P. A.; Bauer, B.; Singer, S. J. *J. Am. Chem. Soc.* **1978**, *100*, 5085.
(5) These clusters have a diameter of about 8.2 Å, with the distance between oppositely situated amino groups being about 25 Å (i.e., total cluster diameter).
(6) Yang, H.; Frey, P. A. *Biochemistry* **1984**, *23*, 3863 and references cited therein.
(7) Kuhn, E.; Fuchs, M.; Varkey, J.; Beer, M. *Proceedings of EMSA Forty-Second Annual Mts.*; Detroit, MI, 1984. Safer, D.; Hainfield, J.; Wall, J. S.; Reardon, J. E. *Science (Washington)* **1982**, *218*, 290.
(8) Ho, R. K. C.; Klemperer, W. G. *J. Am. Chem. Soc.* **1978**, *100*, 6772.
(9) Knoth, W. *J. Am. Chem. Soc.* **1979**, *101*, 759.
(10) Pope, M. T. *Heteropoly and Isopoly Oxometalates*; Springer-Verlag: New York, 1983; p 125.
(11) Dawson, B. *Acta Crystallogr.* **1953**, *6*, 113. D'Amour, V. H. *Acta Crystallogr.; Sect. B: Struct. Crystallogr. Cryst. Chem.* **1976**, *32*, 729.
(12) Lundblad, R. L.; Noyes, C. M. *Chemical Reagents for Protein Modification*; CRC Press: Boca Raton, FL, 1984. Means, G. E.; Feeney, R. E. *Chemical Modification of Proteins*; Holden-Day: San Francisco, CA, 1971.

0002-7863/86/1508-7951$01.50/0